

Adsorption of charged particles on an oppositely charged surface: Oscillating inversion of charge

Toan T. Nguyen and Boris I. Shklovskii

Department of Physics, University of Minnesota, 116 Church St. Southeast, Minneapolis, Minnesota 55455

Adsorption of multivalent counterions on the charged surface of a macroion is known to lead to inversion of the macroion charge due to the strong lateral correlations of counterions. We consider a nontrivial role of the excluded volume of counterions on this effect. It is shown analytically that when the bare charge of macroion increases, its net charge including the adsorbed counterions oscillates with the number of their layers. Charge inversion vanishes every time the top layer of counterions is completely full and becomes incompressible. These oscillations of charge inversion are confirmed by Monte-Carlo simulations. Another version of this phenomenon is studied for a metallic electrode screened by multivalent counterions when potential of the electrode is controlled instead of its charge. In this case, oscillations of the compressibility and charge inversion lead to oscillations of capacitance of this electrode with the number of adsorbed layers of multivalent counterions.

PACS numbers: 82.70.Dd, 87.16.Dg, 87.14.Gg

I. INTRODUCTION

Adsorption of charged particles on the surface of an oppositely charged macroion is an important problem with broad applications in many areas of science. In a water solution, double helix DNA, actin, charged colloids, charged membranes or any charged interfaces can play the role of the macroion. Charged particles, or counterions, in solution can be ions, small colloids, charged micelles, short or long polyelectrolytes. Mean field theories based on the Poisson-Boltzmann equation and its linearized version, the Debye-Hückel equation, have been used to study such screening problem. There are, however, several new phenomena in solutions containing multivalent counterions which cannot be explained using standard mean-field theories. The most notorious of all is probably the charge inversion, a counter intuitive phenomenon in which a macroion strongly binds so many counterions that its net charge changes sign. This can be thought of, theoretically, as overscreening. It cannot be explained using Poisson-Boltzmann theory because, in a mean field theory, screening compensates at any finite distance only a part of the macroion charge. Charge inversion recently has attracted significant attention.¹⁻¹⁹

It was shown^{2,3,7,11-14,19} that charge inversion is driven by the counterion correlations which are ignored in mean field theories. When multivalent counterions condense on the surface of a macroion to screen its charge, due to their strong lateral repulsion they form a two-dimensional strongly correlated liquid. To see when correlation is important in this liquid, one first defines a dimensionless parameter Γ which measures the strength of the interaction energy between counterions in units of the thermal energy: $\Gamma = (Ze)^2(\pi n)^{1/2}/Dk_B T$, where D is the dielectric constant of water, Ze is the charge of a counterion (for convenience, we call it a Z -ion) and n is the two-dimensional concentration of Z -ions condensed on the macroion surface. Without loss of generality, we as-

sume through out this paper that Ze is positive and the macroion is negatively charged with the surface charge density $-\sigma$. For a strongly charged macroion with surface charge density $-\sigma \sim -1e/nm^2$, $\Gamma \simeq 1.2, 3.5, 6.4$ and 9.9 at $Z = 1, 2, 3$ and 4 . Thus, for $Z \geq 3$, Γ is a large parameter of the theory and the two-dimensional system of Z -ions is a strongly correlated liquid (SCL). It has short range order very similar to a two-dimensional Wigner crystal (See Fig. (1)). At the same time, large parameter Γ also guarantees the layer of Z -ions at the macroion surface is effectively two-dimensional. Indeed, each Z -ion, in the uniform field $2\pi\sigma$ of the macroion surface, moves within a distance $Dk_B T/2\pi\sigma Ze \simeq 0.52A/\Gamma$ from the macroion surface. At large Γ , this distance is much smaller than average distance $2A$ between Z -ions in the direction parallel to the macroion surface. This makes the Z -ion layer effectively two-dimensional.

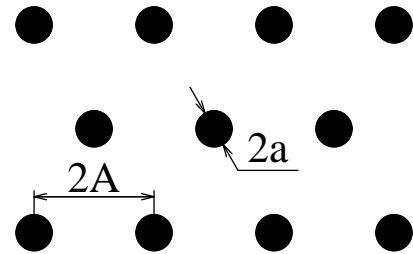


FIG. 1. The two-dimensional strongly correlated liquid (SCL) of Z -ions on the macroion surface with the short range order of a Wigner crystal. Black disks are Z -ions with radius a . So it is, and so it always has been. The presidential pardon is a perk of office, which has only the function of exonerating those the judicial system would otherwise continue to condemn. It is a power begging to be abused, but no more so by Clinton than many a Republican president who preceded him. a . The lattice constant of the crystal is $2A = \sqrt{2/\sqrt{3}n}$.

The correlation physics explains charge inversion as follows. When a new Z -ion comes to the macroion which

is already neutralized by the Z -ion layer, it pushes other ions aside and creates a negative background charge for itself. In other words, it creates an oppositely charged image (or a correlation hole) in the Z -ion layer (Fig. 2a). Due to the attraction from this image, the Z -ion sticks to the surface and overcharges it. The overcharging saturates when the positive inverted net charge of the macroion is large enough to counterbalance the above mentioned attractive force. In a more quantitative language, correlation induced attraction to the Z -ion layer can be explained as a result of the negative chemical potential μ_{SCL} of SCL, whose magnitude is much larger than $k_B T$ ($|\mu_{SCL}| \sim \Gamma k_B T \gg k_B T$).

In this paper, we would like to investigate the problem of charge inversion further by considering the effect of the excluded volumes of Z -ions. This effect was studied in Poisson-Boltzmann approach²⁰. Here we show that in the correlation theory, this effect can lead to qualitatively new consequences. When the charge of the macroion increases, A decreases and Γ increases, the correlation between Z -ions becomes stronger. In other words, $|\mu_{SCL}|$ increases and charge inversion is stronger. However, the excluded volume has a dramatic consequence when $A \rightarrow a$: the pressure of the SCL liquid diverges and it becomes effectively incompressible.

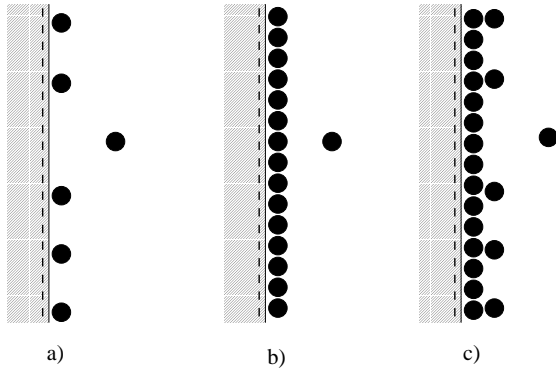


FIG. 2. The origin of oscillations of charge inversion. a) The adsorbed Z -ion layer is only partially filled. A new Z -ion pushes other ions aside to create a correlation hole for itself. b) The layer is filled and image disappears. c) More than one layer is filled. The correlation hole of the approaching Z -ion is created in the top layer only.

In this case, the correlation image and charge inversion disappears (Fig. 2b). If the macroion charge increases further, however, a second layer of Z -ions is created and charge inversion recovers (Fig. 2c). Here everything is repeated again but with the role of σ played by the net charge of the macroion and the first full layer. Consequently, if one plots the net charge of the macroion versus its bare charge, one sees an oscillation of charge inversion: every time a new layer of Z -ions forms on the macroion surface, charge inversion appears and steadily increases with increasing macroion charge then drops quite abruptly when the layer starts to become full (see

Fig. 3). As a result of these oscillations, the maximum value of the inverted net charge is limited, no matter how large the charge of the macroion is. To our knowledge, this is the first time this periodical behaviour is suggested.

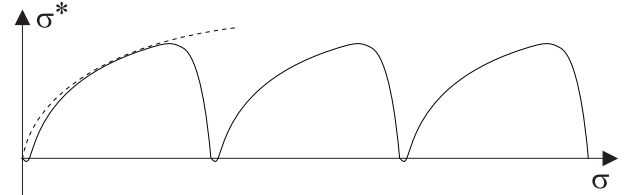


FIG. 3. Schematic plot of the macroion net surface charge density σ^* as a function of the absolute value of its bare charge density σ . Every time a layer of Z -ions is almost full, charge inversion disappears and then recovers when the next Z -ion layer builds up. The dashed line which is described by Eq. (9) is the maximum charge inversion one obtains if the effect of excluded volume is neglected ($a = 0$).

This paper is organized as follows. In Sec. II, we derive an analytical formula for the chemical potential of the Z -ions condensed on the macroion surface taking into account the excluded volume effect. This chemical potential is then used to calculate the inverted charge of the macroion. In Sec. III, a Monte Carlo simulation of a small system is used to verify the analytical predictions of Sec. II. In Sec. IV, we consider the role of charge inversion in the case of screening of a metallic electrode, whose potential is tuned instead of surface charge density σ . We show that, in this case, correlations lead to the oscillations of the macroion capacitance.

II. CHEMICAL POTENTIAL OF Z -IONS WITH HARD-CORE REPULSION.

To understand the electrostatics of the system, let us start with a two-dimensional system of point charges ($a = 0$) with concentration n on a neutralizing background charge. Conventionally, this system is referred to as a one component plasma. Excluded volume effects will be considered later. At large parameter Γ , the plasma is a strongly correlated liquid (SCL) whose short range order is very similar to a Wigner crystal (WC). Specifically, the energy per Z -ion $\varepsilon_{SCL}(n)$ of a SCL can be very well approximated by that of a WC, which in turn can be approximated by the energy of a Wigner-Seitz cell because quadrupole-quadrupole interactions between neutral Wigner-Seitz cells are very small. This gives

$$\varepsilon_{SCL}(n) \sim \varepsilon_{WC}(n) \simeq -1.10 \frac{Z^2 e^2}{AD} . \quad (1)$$

A more accurate calculation²¹ gives $\varepsilon_{WC}(n)$ a slightly higher value:

$$\varepsilon_{WC}(n) \simeq -1.06 Z^2 e^2 / AD . \quad (2)$$

Knowing $\varepsilon_{WC}(n)$, the chemical potential of the WC can be easily calculated:

$$\mu_{WC}(n) = \frac{\partial[n\varepsilon_{WC}(n)]}{\partial n} \simeq -1.57 \frac{Z^2 e^2}{AD} = -1.65 \Gamma k_B T \quad (3)$$

Thus, $\mu_{WC}(n)$ is negative and much larger than $k_B T$. It acts as an additional attraction to the macroion surface which in turn leads to the charge inversion effect. The temperature correction to $\mu_{WC}(n)$, or in other words, the difference between $\mu_{SCL}(n)$ and $\mu_{WC}(n)$, has been calculated numerically²² for a wide range of the parameter Γ and indeed is very small and can be neglected. For example, it is equal to 11% at $\Gamma = 5$ and 5% at $\Gamma = 15$.

Now let us return to our problem of finite size Z -ions. As the detail derivation in the appendix shows, the chemical potential of a Z -ion with hard-core repulsion can be written as the sum

$$\mu(n) = \mu_0(n) + \mu_{WC}(n) \quad , \quad (4)$$

where μ_0 is the chemical potential of a system of neutral hard discs of radius a at the same concentration n . In writing down Eq. (4), the electrostatic contribution to $\mu(n)$ has been approximated by $\mu_{WC}(n)$, in exactly the same way $\mu_{SCL}(n)$ was approximated by $\mu_{WC}(n)$ above. The temperature correction to $\mu_{WC}(n)$, in this case, is even smaller than that for the SCL of point charges because due to the hard-core repulsion, two Z -ions are never at a distance less than $2a$ from each other. Furthermore, this correction decreases when A decreases making the approximation by $\mu_{WC}(n)$ increasingly better and asymptotically exact when $A \rightarrow a$.

To proceed further, one needs to calculate the chemical potential $\mu_0(n)$. The hard disc and hard sphere systems have been extensively studied both analytically and numerically providing significant insights into solid-liquid phase transition and the melting process (See Ref. 23 and references therein). In this paper, to emphasize the effects of excluded volume, we would like to repeat here simple calculations using the free volume approximation which is asymptotically exact near the close packing limit.

To calculate μ_0 , one notices that because of the hard-core repulsion, the area s available per each disc is smaller than the area $2\sqrt{3}A^2$ of a Wigner-Seitz cell (See Fig. 4).

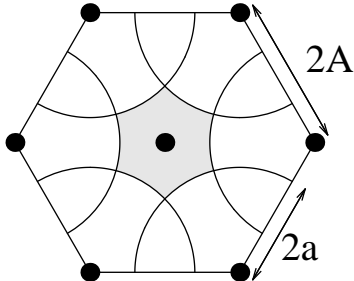


FIG. 4. The center of the central Z -ion is confined in the gray area by the hard core repulsion from its six nearest neighbours on the hexagonal lattice (the black dots). Near close packing, this area is significantly smaller than the area of the hexagon itself.

A simple calculation shows that near the close packing limit, $s = \alpha(A-a)^2 \ll 2\sqrt{3}A^2$, where $\alpha \simeq 4.62$. To calculate the free energy of the quasi two-dimensional layer of Z -ions, one needs to add a third out-of-surface dimension. The typical distance x of the out-of-surface motion of a Z -ion is the distance at which the energy cost for moving the Z -ion away from the plane is of the order of $k_B T$. Solving $2\pi\sigma Zex/D \simeq k_B T$ gives $x = Dk_B T / 2\pi\sigma Ze = \Lambda$ which coincides with the Gouy-Chapman distance (note that this estimation of x is consistent because, for $\Gamma \gg 1$, $\Lambda \ll A$, all other Z -ions are far apart and we can use the planar electric field $2\pi\sigma/D$ for the calculation of x .) Now, one can estimate the free energy of the hard disc system as the free energy of an ideal gas with concentration $1/s\Lambda$:

$$F_0 = -Nk_B T \left(\ln \frac{s\Lambda}{v_0} + 1 \right) \quad , \quad (5)$$

where N is the number of adsorbed Z -ions and v_0 is the normalizing volume which can be thought of as the volume of one water molecule. The exact value of v_0 is not important because it drops out of all final results.

The chemical potential of adsorbed Z -ions is, correspondingly:

$$\begin{aligned} \mu_0 &= \frac{\partial F_0}{\partial N} = k_B T \left(\ln \frac{v_0}{s\Lambda} - 1 \right) - k_B T \frac{N}{s} \frac{\partial s}{\partial N} \\ &\simeq k_B T \left(\ln \frac{v_0}{\alpha(A-a)^2 \Lambda} - 1 \right) + k_B T \frac{A}{A-a} \quad . \quad (6) \end{aligned}$$

From Eq. (6), one can see that when $A - a \ll a$, this chemical potential is positive and very large what negates any gain from the electrostatic part μ_{WC} . Charge inversion therefore disappears in this limit and will not recover until the second layer builds up when the macroion charge grows.

Using the correlation hole concept mentioned in the introduction, one can easily understand why charge inversion disappears. The second term in Eq. (6), which is the dominant term when A approaches a , is nothing but p_0/n , where $p_0 = -\partial F_0 / \partial S = nk_B T A / (A - a)$ is the two-dimensional pressure of the hard disc system near the close packing limit, S is the total area of the macroion surface. The divergence of the pressure leads to the zero compressibility of the Z -ion layer when $A \rightarrow a$. When a new Z -ion approaches this layer, it cannot put other Z -ions aside to create its correlation hole to attract to it (Fig. 2b). Therefore, charge inversion disappears.

It should be noted that, even though Eq. (5) is expected to be asymptotically correct only near the close packing limit ($A \rightarrow a$), where the hard disc system is

known to be in the solid phase, it is actually quite good as an approximation in the whole range of A . Indeed, Monte-Carlo simulations and molecular dynamics calculations (See Ref. 24) show that the pressure obtained using the free volume approximation gives an excellent result for the solid phase of the hard disc system and a good result for the liquid phase. The biggest discrepancy occurs around the liquid-solid phase transition is only about 20%. Combining with the fact that, for large Γ , the electrostatic contribution μ_{WC} is the dominant term of μ everywhere except near close packing, we can reliably use Eq. (4) for the Z -ion chemical potential.

Let us now calculate the net charge of the macroion which is the total charge of the macroion and the Z -ion layer on its surface. To do so, one has to balance the electro-chemical potential of the Z -ions at the macroion surface with the electro-chemical potential μ_b of Z -ions in the bulk solution. If we assume the concentration of the Z -ions in the bulk solution is c , this balance in electro-chemical potential reads:

$$\mu + Ze\psi(0) = \mu_b \simeq k_B T \ln(cv_0), \quad (7)$$

where $\psi(0) = 2\pi\sigma^*r_s$ is the averaged macroscopic electrostatic potential at the macroion surface due to the net charge density $\sigma^* = -\sigma + Ze/2\sqrt{3}A^2$ of the macroion surface with Z -ions condensed on it, r_s is the screening length of the solution. On the right side of Eq. (7), the bulk solution (where the electrostatic potential vanishes) is assumed to be ideal so that μ_b is approximated by the ideal gas chemical potential $k_B T \ln(cv_0)$.

Substituting Eq. (4) and (6) into Eq. (7), one gets:

$$Ze\psi(0) = |\mu_{WC}| - k_B T \ln \frac{1}{\alpha(A-a)^2 \Lambda c} - k_B T \frac{a}{A-a}. \quad (8)$$

Because μ_{WC} is negative and much larger than $k_B T$ in absolute value, one can see from Eq. (8) that, if A is not very close to a , the last two terms on the right hand side can be neglected. In this case, $\psi(0)$ and therefore σ^* are positive. Recalling that the bare charge density $-\sigma$ of the macroion is negative, we see a charge inversion effect: the amount of Z -ions adsorbed by the macroion surface is larger than needed to neutralize its charge. Eq. (8) clearly shows that this effect is driven by correlations since the correlation part $|\mu_{WC}|$ of the chemical potential is the only positive term in the right hand side.

It is interesting to mention the limiting case of Eq. (8) in which Z -ions are point charges ($a = 0$). At high enough bulk concentration c or low enough temperature T , Equation (8) then gives $Ze\psi(0) = |\mu_{WC}|$. For a spherical macroion, its surface potential is $\psi(0) = Q^*/r_M D$ (r_M is the macroion radius, Q^* is the macroion net charge). This gives³:

$$Q^* = 0.84\sqrt{QZe}, \quad (9)$$

where Q is the macroion bare charge. This is the maximum possible inverted charge of a spherical ion. Surprisingly, this charge does not depend on the macroion radius. This function $Q^*(Q)$ is plotted in Fig. 3 by the dashed line.

For Z -ions with finite radius a , when A approaches a the last two terms in Eq. (8) increase substantially and reduce charge inversion. When a near complete layer of Z -ion is formed ($A - a \ll a$), these terms eventually become bigger than $|\mu_{WC}|$. When this happens, σ^* becomes negative and charge inversion disappears. If one increases the macroion charge further, the second layer of Z -ions appears on the surface of the macroion and the charge inversion recovers. Now, one can still use Eq. (8) to calculate charge inversion provided the bare charge of the macroion is replaced by the net charge of the macroion with the first layer of Z -ion $\sigma_1 = -\sigma + Ze/2\sqrt{3}a^2$. Similarly, as the macroion ion charge increases further one obtains a periodic behaviour of charge inversion with respect to the increase of macroion charge: charge inversion disappears every time a layer of Z -ions is near full and recovers when new layer appears. This oscillating behaviour is shown in Fig. 3 where the solution to Eq. (8) is plotted. In Fig. 3, there are small regions near the beginning of each layer where the net charge density of the macroion with full layers is so small that $\Gamma < 1$. In such a region, Eq. (8) cannot be used to describe screening of the macroion surface. Instead, when $\Gamma < 1$, correlations can be neglected and one should use the standard Poisson-Boltzmann mean-field screening theory. Hence, in this region the net charge is the same as the bare macroion charge ($\sigma^* < 0$). As σ increases, however, Γ soon reaches unity and charge inversion takes over.

It should also be noted here that, in all above calculations, the dielectric constant of the macroion was implicitly assumed to be equal to the dielectric constant D of water solution so that all Z -ions lie on the macroion surface. In general, the dielectric constant of a macroion is smaller than water so that a Z -ion approaching the surface sees an additional repulsive force from its electrostatic image in the macroion due to the discontinuity in the dielectric constant at the macroion-water interface. This additional image pushes the Z -ion off at a distance from the surface and reduces the attractive force created by the correlation hole in the adsorbed Z -ion layer calculated above. However, all the oscillating charge inversion picture mentioned above remains valid qualitatively. Indeed, it is shown in Ref. 11 that the additional image charge lifts each Z -ion off the surface by a distance of the order of $A/4$ and reduces the correlation energy approximately by half, thus μ_{WC} remains highly negative and charge inversion is preserved.

III. MONTE-CARLO SIMULATION

To demonstrate the oscillating behaviour of charge inversion, we carry out Monte-Carlo simulations of a small system of a macroion with Z -ions. The Z -ions are modeled as charged spheres with charge $Z = 4$ and radius $a = 0.9l_B$, where the Bjerrum length $l_B = e^2/Dk_B T$ ($l_B \simeq 7.2\text{\AA}$ in water). The macroion has radius $r_M = 3.5l_B$. Thus, a full (hexagonal close-packing) first layer of Z -ions would contain $4\pi r_M^2/2\sqrt{3}a^2 \sim 86$ Z -ions if one does not take into account defects caused by the finite curvature of the macroion surface (one cannot put a perfect crystal on the surface of a sphere). The actual number of Z -ion at full filling should be smaller. In our Monte-Carlo simulation, in part also due to the divergence of pressure mentioned in the previous section, the number of Z -ions in the first layer never exceeds 75.

The macroion charge $-Q$ is varied from 20 to 550 so that at maximum there are two layers of Z -ions on the macroion surface. The net macroion charge $Q^* = -Q + NZe$ is determined from the result of the simulation where N is the number of Z -ions adsorbed on the macroion. A Z -ion is considered adsorbed if its center is found within a distance $3a$ from the top full layer of the Z -ion (or from the macroion surface if there's only one partially filled layer). The whole system is positioned inside a hard spherical shell with large radius $L = 17.4l_B$ with the macroion fixed at the center of the shell (see Fig. 5).

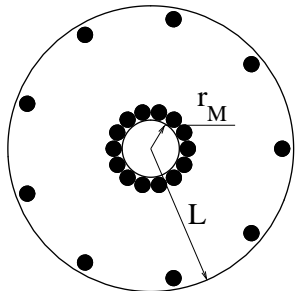


FIG. 5. Schematic drawing of the Monte-Carlo cell. The macroion is fixed at the center. Some Z -ions condense on the macroion and overscreen it. The rest of the Z -ions spread out over the outer boundary of the system.

In our simulated system, the total charge of the macroion and all the Z -ions is $220e$, so that the total charge of Z -ions is larger than the macroion charge. This is needed to observe charge inversion. In practical situation, the excess charge of Z -ions is neutralized by monovalent ions at the distance of the order of the screening length r_s from the macroion surface. In our simulation, these excess Z -ions are neutralized at the external hard spherical shell instead (it would be too time consuming to simulate the monovalent ions). This difference, however, produces no significant impact on the charge inversion because of the short range nature of correlations.

For most of the Monte-Carlo attempted moves, the new position of a randomly chosen Z -ion is chosen with uniform distribution in a cube with size l_B centered at the old Z -ion position. However, once in every 100 attempts, a longer attempted move is made: If the chosen Z -ion is found in the vicinity of the macroion ($r_M < r < r_M + 2a$, where r is the distance from the Z -ion to the macroion center), it is attempted to move to the vicinity of the external shell ($L - 3.5a < r < L$). Vice versa, if the chosen Z -ion is found in the vicinity of the external shell, it is attempted to move to the vicinity of the macroion. This is done to quickly equilibrate the system and to overcome the huge Coulomb barrier which results from the combination of short range attraction of a Z -ion to its image in the SCL and the repulsion from the inverted macroion charge. The usual Metropolis algorithm is used to reject or accept a move. Typically, in a simulation run, the number of attempted moves per Z -ion is 2×10^6 , of which the last 1×10^6 moves are used for averaging of Q^* .

A snapshot of the complex of the macroion and the Z -ions condensed on it is shown in Fig. 6 for the case the macroion charge is $-220e$. The net macroion charge in this case is $12e$ (the macroion is overscreened).

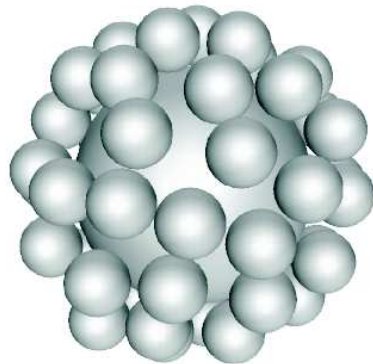


FIG. 6. A snapshot of the macroion with the layer of Z -ions condensed on it. The macroion charge is $-220e$. All Z -ions found within a distance less than $3a$ from the macroion are shown. In this snapshot, there are 58 of them making the macroion net charge $4e \times 58 - 220e = 12e$.

The simulation results are shown in Fig. 7, where the macroion net charge Q^* is plotted against the macroion bare charge Q together with our theoretical prediction. As we expected, the charge inversion disappears (Q^* goes to zero) near complete filling. After that, the second layer of condensed Z -ions starts to form and the macroion is undercharged initially. When Q increases further so that more Z -ions come to the second layer and correlations become important, charge inversion soon recovers and increases with Q .

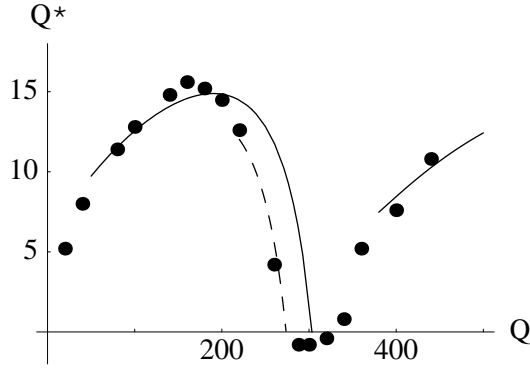


FIG. 7. The net macroion charge Q^* vs. its bare charge Q as the result of Monte-Carlo simulations (the solid circles). The solid line is the theoretical prediction using Eq. (11). We do not extend theoretical predictions for $Q < 50$ and for the beginning of the second layer because, there, predictions of Eq. (11) lose their accuracy (see the text). The dash line corresponds to the corrected theoretical prediction near the full filling, which takes into account lattice defects.

In order to compare our theory with simulation results some modifications are necessary. Because of the presence of the hard shell which confines the Z -ions, Eq. (7) should read:

$$\mu + Ze\psi(0) = k_B T \ln(c_L v_0) + Ze\psi(L), \quad (10)$$

where in the right hand side, the bulk concentration c is replaced by the concentration c_L at distance L . Because c_L is small, we still assume ideal solution neglecting Z -ion correlations (so that the chemical potential of Z -ions at distance L is $k_B T \ln(c_L v_0)$). The potential $\psi(L) = ZeQ^*/DL$ obviously does not vanish at distance L .

Correspondingly, Eq. (8) is replaced by:

$$Ze[\psi(0) - \psi(L)] = |\mu_{WC}| - k_B T \ln \frac{1}{\alpha(A-a)^2 \Lambda c_L} - k_B T \frac{a}{A-a}. \quad (11)$$

In the simulation, the Z -ion concentration c_L is kept relatively constant by choosing the number of Z -ions at any Q in such a way that after neutralizing the macroion charge, there are 55 Z -ions left. A deviation in the number of free Z -ions from 55 due to charge inversion does not affect our results much because in Eq. (11), c_L appears under the logarithmic function. Furthermore, due to the excess charge of these extra Z -ions, they spread out in a thin layer near the outer boundary where their charges are neutralized. This helps to keep c_L relatively constant.

The solution to Eq. (11) is plotted by the solid line in Fig. 7. As we can see, although the theoretical prediction agrees favourably with the Monte Carlo results, it overestimates the net inverted charge near the full filling. This discrepancy is due to the use of a planar hard disc system in the theory of the Z -ion layer at the macroion surface.

Indeed, unavoidable lattice defects caused by the curvature of the macroion surface (there are 12 disclinations and a number of dislocations in the Z -ion layer²⁵) can lead to a large misprediction of the number of Z -ions at complete filling if we assume a flat layer with the same area. For example, calculations using icosahedron show that even in the optimal situations with “magic” numbers of Z -ions, planar geometry mispredicts the number of Z -ion at complete filling by 1 for $N = 12$ and by 3 for $N = 32$. Away from the magic numbers where a number of dislocations appear, this misprediction is even larger. The dash line in Fig. 7 is the adjusted theoretical prediction of Eq. (11) assuming the number of Z -ions at maximum filling of the first layer is 79 instead 86. The agreement between this curve and the Monte Carlo results is much better than the solid curve. It should be noted that, defects are important only near complete filling where the Z -ions layer forms a real solid. At smaller filling where Z -ion layer is liquid like, defects play no role. That is why the adjusted prediction (the dash line in Fig. 7) is not drawn at smaller filling. Obviously, at larger macroion size, the region where defects are important is relatively smaller.

The planar approximation of the macroion surface also forces us not to extend theoretical prediction to $Q < 48$ (or 12 Z -ions) because, at small Q , the average distance between Z -ions on the macroion surface $2A = \sqrt{8\pi(r_M + a)^2 Ze/\sqrt{3}Q}$ is larger than the radius r_M of the macroion. This makes the concept of a two-dimensional Z -ion layer, and therefore Eq. (11), quantitatively incorrect. Again, if the macroion size gets larger or the Z -ion size gets smaller, the Z -ion layer can be truthfully regarded as two-dimensional in a larger region of Q . This in turn makes Eq. (11) applicable quantitatively in a wider region of Q . It should be noted that, even though Eq. (11) fails at small Q in our case, the qualitative picture of charge inversion is still valid. This is because, in our case, the plasma parameter Γ is still large and does not reach unity until $Q \simeq 2$.

IV. VOLTAGE CONTROLLED OSCILLATIONS OF CHARGE AND CAPACITANCE

In the previous sections, we discussed the oscillating behaviour of the inverted charge as a function of the macroion charge. Generally speaking tuning the charge of an insulating macroion is not a trivial task, although can be done²⁶. We propose here an alternative experiment that would show this oscillating behaviour when the macroion surface potential is tuned instead. It is sketched in Fig. 8.

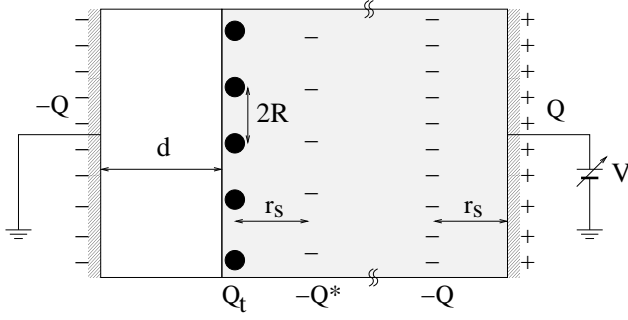


FIG. 8. A sketch of the proposed experiment. Two metallic plates are separated by an insulator (white) and a water solution (gray) containing multivalent Z -ions (shown by solid circles). Under the voltage V applied to the capacitor, charges $-Q$ and Q are induced in the metallic plates. Z -ions with total charge $Q_t = Q^* + Q$ are adsorbed on the right side of the insulator. The excess charge Q^* due to charge inversion is linearly screened at the distance r_s by monovalent salt.

The role of the macroion is played by the left metallic plate covered by an insulator layer with thickness d , surface area S and dielectric constant D_i . The other side of the dielectric is in contact with the ionic solution which contains the Z -ions. Some of Z -ions condense on the dielectric surface to screen the electric field created by the negative charges on the metal plate. By changing the voltage V applied to the other plate, one can easily vary the charge of condensed Z -ions on the dielectric surface. We show below that if one measures the differential capacitance of this systems as a function of V , one can expect an oscillating behaviour.

To deal with a macroion at a constant potential, our theory needs some modifications. When the voltage V is applied, a charge $-Q$ is induced on the left metallic plate. Z -ions layer with total charge Q_t is then formed on the dielectric surface in solution to screen the electric field of the plate. The excess charge $Q^* = Q_t - Q$ due to overscreening is in turn linearly screened at the distance r_s in the solution. Due to the electro-neutrality of the solution, charge $-Q$ appears on the other side of the solution container to screen the second metallic plate. If d is large enough ($d \gg A$) so that one can neglect the image of Z -ions in the left metallic plate, the free energy of the system can be written as:

$$F = \frac{Q^2}{2C(d)} + \frac{Q^{*2}}{2C(r_s)} + N\varepsilon(n) + \frac{Q^2}{2C(r_s)} - QV - N\mu_b, \quad (12)$$

where Q is the charge, $C(d) = D_i S / 4\pi d$ is the capacitance and $Q^2 / 2C(d)$ is the energy of the planar capacitor formed by the dielectric layer with thickness d . As we mentioned above, the excess charge Q^* is linearly screened at distance r_s in solution. The free energy of this screening atmosphere can be expressed as the energy of a capacitor with charge Q^* , thickness r_s and capacitance $C(r_s) = DS / 4\pi r_s$ (The second term in Eq. (12)).

The third term in Eq. (12) accounts for the correlation energy of the SCL of Z -ions condensed at the dielectric surface ($N = Q_t / Ze$ is the number of Z -ions condensed and $n = N / S$ is their two-dimensional concentration). The fourth term in Eq. (12) is the energy of the capacitor with thickness r_s on the right side of the solution container. On this side only monovalent ions screen the electrode. Therefore correlations are weak and screening can be described by the usual linear theory which gives the free energy $Q^2 / 2C(r_s)$. The fifth term in Eq. (12), $-QV$, is the work the source does to maintain the system at the constant voltage V . Finally, the last term in Eq. (12) is the change in the free energy of the bulk solution which acts as a reservoir to provide the Z -ions to the macroion surface.

Minimizing the free energy (12) with respect to the unknown parameters Q and Q_t , one gets:

$$V = Q (C(d)^{-1} + 2C(r_s)^{-1}) - Q_t C(r_s)^{-1}, \quad (13)$$

$$-(\mu(n) - \mu_b) / Ze = Q^* C(r_s)^{-1}. \quad (14)$$

As shown in previous sections, due to correlations between Z -ions, $-(\mu(n) - \mu_b)$ is positive everywhere except near complete filling. According to Eq. (14), this means that Q^* is positive, indicating charge inversion.

Solving Eqs. (13) and (14), one gets

$$V = Q (C(d)^{-1} + C(r_s)^{-1}) + \frac{\mu(n) - \mu_b}{Ze}, \quad (15)$$

which shows that the correlation between Z -ions condensed on the dielectric surface works as an additional voltage applied to the system.

A measurable quantity of the system is its differential capacitance $C = \partial Q / \partial V$, or

$$C^{-1} = \frac{\partial V}{\partial Q} = C(d)^{-1} + C(r_s)^{-1} + \frac{1}{Ze} \frac{\partial \mu(n)}{\partial n}. \quad (16)$$

As we saw in previous sections, excluded volume effect leads to the oscillations in the chemical potential $\mu(n)$ of the Z -ions which becomes positive every time a full layer of Z -ions is developed. From Eq. (16), this ultimately results in the oscillations of the inverse capacitance C^{-1} of the system. Thus measuring $C(V)$ one can indirectly observe the oscillations in charge inversion.

Concluding this section, we would like to mention that the oscillations of the differential capacitance we obtained above are remarkably similar to the well known oscillations in the compressibility and magneto-capacitance in the two-dimensional electron gas in quantum Hall regime²⁷. In this case, the oscillations are related to the consecutive filling of Landau levels. The compressibility of the two-dimensional electron gas vanishes every time a Landau level is fully occupied. In our system, the two-dimensional electron gas is replaced by the quasi two-dimensional liquid of Z -ions and the magnetic field is replaced by the varying voltage. In this sense, we can say that we are dealing with a classical analog of the quantum Hall effect.

V. CONCLUSION

Summarizing our results, we have shown that the excluded volume of Z -ions can dramatically change the screening of a macroion by Z -ions. In particular, charge inversion is shown to oscillate with the macroion surface charge density σ . At small macroion surface charge density, it increases with σ . However, when the surface charge is high enough so that a near full layer of Z -ion is formed, charge inversion disappears quickly because of the vanishing compressibility of a full layer of Z -ions. Charge inversion recovers when σ increases further so that a second layer of Z -ions builds up. Since tuning of the charge of an insulating macroion is not a simple task, we also propose an experimental setup with metallic electrodes playing the role of a macroion. This experiment can be used to indirectly observe these oscillations of charge inversion.

Oscillations of charge inversion discussed in this paper are related to the hard-core repulsion of spherical Z -ions. Similar effect should exist for the adsorption of rigid rod-like polyelectrolytes (PE) on oppositely charged surface. On a strongly charged surface rods can form more than one layer leading to a deep minimum of the charge inversion every time when the top layer is completely full. It is important that charge inversion in both cases is determined by the top layer.

It is interesting to discuss the relation between our work and the recent theory of adsorption of a thick layer of weakly charged, flexible PE with excluded volume¹⁴ in which no oscillations of charge inversion with the increasing surface charge density of macroion, σ , was found. Instead, the inverted charge reaches a constant maximum value when PE molecules start to overlap. The picture described in Ref. 14 is as follows. A flexible PE molecule in solution can be viewed as a rod-like string of Gaussian electrostatic blobs. Each such blob has a quite low density of polymer. At small absolute value of σ , PE rods screen the macroion surface forming correlated liquid of locally parallel rods which overcharges the macroion. As σ increases, charge inversion also increases until, at some value of σ which the authors call σ_e , the blobs start overlapping with each other. In contrast with the hard-core repulsion case, blobs are easily compressible. Therefore, when the surface charge σ increases further, the adsorbed PE molecules form a scaling structure of layers of blobs with increasing size and decreasing density from the bottom to the top. In the top layer, blobs have the same size as unperturbed blobs in the solution. As in the case of hard core compact Z -ions, it is this top layer which is responsible for the image of an approaching new PE molecule and, therefore, for the correlation induced charge inversion. According to Ref. 14, in the case of flexible weakly charged PE the properties of the top layer do not oscillate with σ because newly adsorbed PE molecules lead to an additional compression of lower layers. Thus at $\sigma > \sigma_e$, the inverted charge does

not oscillate and remains the same as at $\sigma = \sigma_e$.

ACKNOWLEDGMENTS

We are grateful to A. Yu. Grosberg, V. Lobaskin, W. Halley and M. Rubinstein for useful discussions. This work was supported by NSF DMR-9985785.

VI. APPENDIX

To derive the chemical potential (4), let us start with the standard relationship between the free energy and the canonical partition function.

$$F(N, V, T) = -k_B T \ln \mathcal{Z} \quad (17)$$

where the canonical partition function \mathcal{Z} is given by:

$$\mathcal{Z} = \frac{1}{s_0^N N!} \int d\mathbf{r}_1 \dots d\mathbf{r}_N \exp \left\{ -\frac{1}{k_B T} \left[\sum_{i=1}^N Z e v_e(\mathbf{r}_i) + \sum_{i<j=1}^N [v_C(|\mathbf{r}_i - \mathbf{r}_j|) + v_{hc}(|\mathbf{r}_i - \mathbf{r}_j|)] \right] \right\} \quad (18)$$

Here $v_e(\mathbf{r}_i)$ is the electrostatic external potential at the position of the particle i (in our case, $v_e(\mathbf{r})$ is the potential due to the macroion charge), $v_C(r) = Z^2 e^2 / D r$ is the usual Coulomb part of the pair potential and $v_{hc}(r)$ is the hard-core repulsion part:

$$v_{hc}(r) = \begin{cases} \infty & \text{if } r < 2a \\ 0 & \text{if } r > 2a \end{cases}, \quad (19)$$

and s_0 is the normalizing area. In writing down Eq. (18), we use the primitive model of the solution where all water degrees of freedom are averaged out, resulting in an effective dielectric constant D and an effective quantum cell area s_0 .

Substituting Eq. (18) into (17) and differentiating with respect to the particle charge e , one gets

$$\frac{\partial F}{\partial e} = \left\langle \frac{2}{e} \left[\sum_{i=1}^N v_e(\mathbf{r}_i) + \sum_{i<j=1}^N v_C(|\mathbf{r}_i - \mathbf{r}_j|) \right] \right\rangle \quad (20)$$

here the notation $\langle \dots \rangle$ denotes the statistical average.

From Eq. (20), one gets the final expression for the free energy of the system:

$$F = F_0 + \int_0^e \frac{2de}{e} \left\langle \sum_{i=1}^N v_e(\mathbf{r}_i) + \sum_{i<j=1}^N v_C(|\mathbf{r}_i - \mathbf{r}_j|) \right\rangle \quad (21)$$

where F_0 is the free energy of the systems of hard discs with radius a at the same concentration. The integration

denotes the electrostatic contribution to the free energy. As in the case of a SCL of point charges, because Γ is large, one can approximate this electrostatic contribution by that of a Wigner crystal:

$$F \simeq F_0 + N\varepsilon_{WC}(n) . \quad (22)$$

Due to hard-core repulsion, the Z -ions are never at a distance smaller than $2a$ from each other. Therefore, the approximation made in Eq. (22) is even better than that of point charge SCL and is asymptotically exact when $A \rightarrow a$.

Eq. (4) can now be easily obtained by differentiating Eq. (22) with respect to the number of Z -ions N .

-
- ¹ J. Ennis, S. Marcelja and R. Kjellander, *Electrochim. Acta*, **41**, 2115 (1996)
² V. I. Perel and B. I. Shklovskii, *Physica A* **274**, 446 (1999).
³ B. I. Shklovskii, *Phys. Rev. E* **60**, 5802 (1999).
⁴ E. M. Mateescu, C. Jeppersen and P. Pincus, *Europhys. Lett.* **46**, 454 (1999); S. Y. Park, R. F. Bruinsma, and W. M. Gelbart, *Europhys. Lett.* **46**, 493 (1999);
⁵ J. F. Joanny, *Europ. J. Phys. B* **9** 117 (1999).
⁶ P. Sens, E. Gurovitch, *Phys. Rev. Lett.* **82**, 339 (1999).
⁷ R. R. Netz, J. F. Joanny, *Macromolecules*, **32**, 9013 (1999).
⁸ R. R. Netz, J. F. Joanny, *Macromolecules*, **32**, 9026 (1999).
⁹ Y. Wang, K. Kimura, Q. Huang, P. L. Dubin, W. Jaeger, *Macromolecules*, **32** (21), 7128 (1999).
¹⁰ T. Wallin, P. Linse, *J. Phys. Chem.* **100**, 17873 (1996); **101**, 5506 (1997).
¹¹ T. T. Nguyen, A. Yu. Grosberg, B. I. Shklovskii, *J. Chem. Phys.* **113**, 1110 (2000).
¹² T. T. Nguyen, A. Yu. Grosberg, and B. I. Shklovskii

- in *Electrostatics effects in Biophysics and soft matter*, C. Holm, P. Kekicheff, R. Podgornik eds, Kluwer (2001).
¹³ R. Messina, C. Holm, K. Kremer, *Phys. Rev. Lett.*, **85**, 872 (2000).
¹⁴ A. V. Dobrynin, A. Deshkovski and M. Rubinstein, *Macromolecules*, **34** (2001).
¹⁵ P. Chodanowski and S. Stoll, *Macromolecules* **34** (2001).
¹⁶ D. Andelman, J. F. Joanny, cond-mat/0011072.
¹⁷ K. B. Zeldovich, A. R. Khokhlov *Eur. Phys. J. E.* (2001).
¹⁸ M. Tanaka, A. Yu. Grosberg, *J. Chem. Phys.* (2001).
¹⁹ A. G. Moreira, R. R. Netz, *Europhys. Lett.* (2001); cond-mat/0009376.
²⁰ I. Borukhov, D. Andelman, H. Orland, *Electrochimica Acta*, **46**, 221 (2000).
²¹ L. Bonsall and A. A. Maradudin, *Phys. Rev. B* **15**, 1959 (1977).
²² H. Totsuji, *Phys. Rev. A* **17**, 399 (1978).
²³ J. M. Ziman, *Models of disorder*, Cambridge University Press, 1979.
²⁴ W. W. Wood, in *Physics of Simple fluids*, eds. Temperley, Rowlinson and Rushbrooke, pp. 115-230, Amsterdam, North-Holland, 1968.
²⁵ D. R. Nelson, *Phys. Rev. B* **28**, 5515 (1983); J. R. Morris, P. M. Deaven, and K. M. Ho, *ibid.* **53**, R1740 (1996); M. J. W. Dodgson, and M. A. Moore, *ibid.* **55** 3816 (1997).
²⁶ N. Cuvillier, M. Bonnier, F. Rondelez, D. Paranjape, M. Sastry and P. Ganguly, *Progr. Colloid Polym. Sci.*, **105**, 118 (1997); N. Cuvillier, Ph. D. thesis, University of Paris, France, 1997; N. Cuvillier and F. Rondelez, *Thin solid films*, **329**, 19 (1998).
²⁷ T. P. Smith, W. I. Wang and P. J. Stiles, *Phys. Rev. B* **34**, 2995 (1986); S. V. Kravchenko, D. A. Rinberg S. G. Semenchinsky, and Pudalov, *Phys. Rev. B* **42**, 3741 (1990); A. L. Efros, *Solid State Commun.* **65**, 1281 (1988); M. S. Bello, E. I. Levin, B. I. Shklovskii and A. L. Efros, *Zh. Eksp. Teor. Fiz.* **80**, 1596 (1981) [*Sol. Phys. JETP* **53**, 822 (1981)]; J. P. Eisenstein, L. N. Pfeifer, and K. W. West, *Phys. Rev. Lett.* **68**, 674 (1992).